Chinese Chemical Letters 36 (2025) 109676

Contents lists available at ScienceDirect

Chinese Chemical Letters

journal homepage: www.elsevier.com/locate/cclet

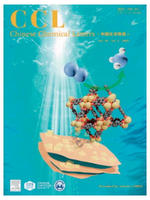

# Porous sorbents for direct capture of carbon dioxide from ambient air

Yuchen Zhang[a], Lifeng Ding[b], Zhenghe Xie[b], Xin Zhang[a,*], Xiaofeng Sui[b], Jian-Rong Li[a]

[a] *Beijing Key Laboratory for Green Catalysis and Separation and Department of Chemical Engineering, College of Materials Science & Engineering, Beijing University of Technology, Beijing 100124, China*
[b] *Beijing Energy Holding Company Limited, Beijing 100022, China*

ARTICLE INFO

*Article history:*
Received 26 December 2023
Revised 23 January 2024
Accepted 22 February 2024
Available online 24 February 2024

*Keywords:*
Direct air capture
Carbon neutrality
Porous materials
Physisorption
Chemisorption

ABSTRACT

Large-scale deployment of carbon dioxide ($CO_2$) removal technology is an essential step to cope with global warming and achieve carbon neutrality. Direct air capture (DAC) has recently received increasing attention given the high flexibility to remove $CO_2$ from discrete sources. Porous materials with adjustable pore characteristics are promising sorbents with low or no latent heat of vaporization. This review article has summarized the recent development of porous sorbents for DAC, with a focus of pore engineering strategy and adsorption mechanism. Physisorbents such as zeolites, porous carbons, metal-organic frameworks (MOFs), and amine-modified chemisorbents have been discussed and their challenges in practical application have been analyzed. At last, future directions have been proposed, and it is expected to inspire collaborations from chemistry, environment, material science and engineering communities.

## 1. Introduction

In recent years, the world has faced serious environmental challenges. With the burning of fossil fuels and the continuous intensification of industrial activities, the emission of $CO_2$ in the atmosphere is constantly increasing, which promoted the global warming effect and extreme climate events [1–4]. Based on current trend, it is predicted that by 2100, the concentration of $CO_2$ in the atmosphere will reach 530–980 ppm, approximately twice of the current 410 ppm level, leading to an increase of global average temperature to 6.1 °C in 2100 [5]. Therefore, many countries have worked on technologies to reduce carbon emission and achieve carbon neutrality. Carbon capture, utilization technologies and sequestration (CCUS) technology is believed to play an important role towards this goal [6,7].

As early as 1999, Lackner proposed the concept of direct air capture (DAC), and is now broadly defined as the direct extraction of $CO_2$ from ambient air, which aims to alleviate atmosphere $CO_2$ concentration [8]. Subsequently, Chichilnisky *et al.* filed a patent on direct air $CO_2$ capture of amine-modified sorbent in 2007 [9]. Compared with $CO_2$ capture at emission sites, the DAC site can be planted flexibly close to the geological storage or catalytic utilization sites (Fig. 1). Besides, it can also avoid the detrimental effect of high concentration acidic impurities from industrial emission source, and the life cycle of sorbents can be significantly elongated [10]. Therefore, DAC is considered as a promising negative emission technology [11]. At present, global DAC factories are operating on a small scale, and 18 DAC facilities have been built in Canada, Europe, and the United States (specific demonstration projects shown in Table 1) [12]. Currently, the operational cost is still relatively high, due to the low concentration of $CO_2$ (410 ppm) in the air, and the development of advanced sorbents and engineering design is needed towards practical application in a large scale.

Over the years, sorbents for $CO_2$ adsorption have developed rapidly. Porous solid sorbents with high specific surface area and tunable pore environment have shown bright prospect as $CO_2$ capture medium [13], as the common issues of amine solution including equipment corrosion, solvent loss and high regeneration cost [14] can be overcome. Based on adsorption mechanism, porous sorbents can be classified as physisorbents and chemisorbents, and the porous structure promoted the adsorption processes in various ways. For physisorbents, the weak interaction between sorbents and sorbates can be significantly enhanced in a porous structure through synergistic binding with multiple sites. Especially, the emerging framework materials such as metal-organic frameworks (MOFs), covalent-organic frameworks (COFs) with finely tunable pore size, shape and surface functionality have enabled the delicate control of host-guest interaction [15]. For chemisorbent, the porous structure would facilitate the mass transportation and promote the adsorption kinetics.

This work summarized the recent development of solid porous sorbents for direct air capture of $CO_2$ including the synthetic strategies, surface modification and performance. The performance

---

[*] Corresponding author.
*E-mail address:* zhang.xin@bjut.edu.cn (X. Zhang).

https://doi.org/10.1016/j.cclet.2024.109676

**Table 1**
DAC plants in operation worldwide.

| Company | Country | Sector | $CO_2$ storage or use | Start-up year | $CO_2$ capture capacity ($tCO_2$/year) |
|---|---|---|---|---|---|
| Global thermostat | United States | R&D | Not known | 2010 | 500 |
| Global thermostat | United States | R&D | Not known | 2013 | 1000 |
| Climeworks | Germany | Customer R&D | Use | 2015 | 1 |
| Carbon engineering | Canada | Power-to-X | Use | 2015 | Up to 365 |
| Climeworks | Switzerland | Power-to-X | Use | 2016 | 50 |
| Climeworks | Switzerland | Greenhouse fertilisation | Use | 2017 | 900 |
| Climeworks | Iceland | $CO_2$ removal | Storage | 2017 | 50 |
| Climeworks | Switzerland | Beverage carbonation | Use | 2018 | 600 |
| Climeworks | Switzerland | Power-to-X | Use | 2018 | 3 |
| Climeworks | Italy | Power-to-X | Use | 2018 | 150 |
| Climeworks | Germany | Power-to-X | Use | 2019 | 3 |
| Climeworks | Netherlands | Power-to-X | Use | 2019 | 3 |
| Climeworks | Germany | Power-to-X | Use | 2019 | 3 |
| Climeworks | Germany | Power-to-X | Use | 2019 | 50 |
| Climeworks | Germany | Power-to-X | Use | 2020 | 50 |
| Climeworks | Germany | Power-to-X | Use | 2020 | 3 |
| Climeworks | Germany | Power-to-X | Use | 2020 | 3 |
| Climeworks | Iceland | $CO_2$ removal | Storage | 2021 | 4000 |

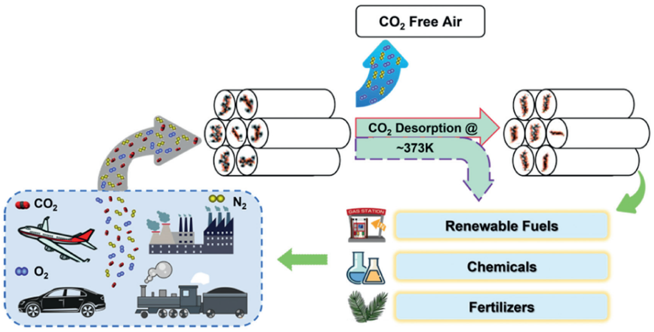

**Fig. 1.** Scheme of DAC and subsequent utilization chain.

and the technical maturity of representative porous sorbents for DAC have been discussed, further we have analyzed their potential for large-scale implementation in the future.

## 2. Physisorption materials

Physical adsorption is usually defined as a form of adsorption in which the target adsorbate is attached to the surface of the sorbent by hydrogen bond, vander Waals force and electrostatic attraction [16]. These sorbent-sorbate interactions are generally weak, so the adsorption process is reversible with fast kinetics. Typical physisorption materials include traditional porous materials such as zeolites, mesoporous silica, carbon-based materials, as well as emerging porous materials such as MOFs [17], porous organic polymers (POPs) [18] and COFs [19].

### 2.1. Zeolites

The introduction of aluminum atoms in the silicate-based of zeolite skeleton leads to the negative charge which is balanced with cations (for example: $Na^+$, $La^{3+}$) acting as Lewis acidic sites [20]. Due to the interaction between the Lewis acidic metal cations and carbon dioxide, selective $CO_2$ adsorption can be realized at lower temperatures [21,22]. The performance of the zeolite can be further regulated by ion exchange and other modification techniques. For example, by doping iron into 13X zeolite through an in-situ crystallization method, Hu *et al.* [23] obtained Fe@13X zeolite with faster adsorption rate and higher adsorption capacity of 0.64 mmol/g compared with the parent zeolite. Later, Hong *et al.* adopted the strategy of introducing a crystal growth inhibitor into a small-pore zeolite to synthesize nanocrystalline molecular sieves (K-CHA) and observed to exhibit a $CO_2$ uptake of 0.7 mmol/g at 298 K, 400 ppm [24]. In order to make zeolite more competitive in future industrial applications, a standard method should be established to evaluate the performance parameters of the sorbent [25], such as adsorption-desorption kinetic analysis [26], recyclability [27], and evaluation at pilot scale [28].

### 2.2. Mesoporous silica

Silicon-based porous materials have become one of the most promising commercial sorbents due to their low cost and easy accessibility of synthetic precursors. Significant efforts have been made to control the pore structure of mesoporous silica. For example, Chen's team used pyrolysis to calcine hollow mesoporous silica to obtain highly dispersed core-shell micro-nano particles, which exhibited capture capacity of 0.75 mmol/g at 0.2 bar and 298 K [29]. While the much lower adsorption capacity under 400 ppm pressure makes it not efficient for DAC application. The low adsorption capacity is due to its weak interaction with $CO_2$. Taking advantage of their high porosity, the surface modification of mesoporous silica is a more appealing strategy which will be discussed in the section of chemisorbents.

### 2.3. Metal-organic framework

MOF materials have drawn great attention in recent years, for their high surface area and tunable pore properties. The pore size can be precisely regulated from ultra-micropore to mesopore range, making them promising candidate for gas storage and separation [30,31]. By controlling the pore structure and the surface functionalization, selective capture of specific gases from complex mixtures have been realized [32,33]. Fig. 2 shows the crystal structure of some representative MOFs of diverse pore size and shape [34].

The adsorption of $CO_2$ by MOF is affected by pore size and surface environment. In order to improve the adsorption capacity of $CO_2$ at low partial pressure, Shekhah *et al.* [17] reported SIFSIX-3-Cu MOF constructed by pillaring a two-dimensional network with silicon hexafluoride anions. Given the micropore size (3.5 Å) and cooperative binding of $CO_2$ through multiple fluoride sites, the material uptakes significant amount of $CO_2$ (1.24 mmol/g) at 298 K and 0.4 mbar. After that, Bhatt *et al.* synthesized NbOFFIVE-1-Ni through replacement of the inorganic pillar in SIFSIX-3-X with

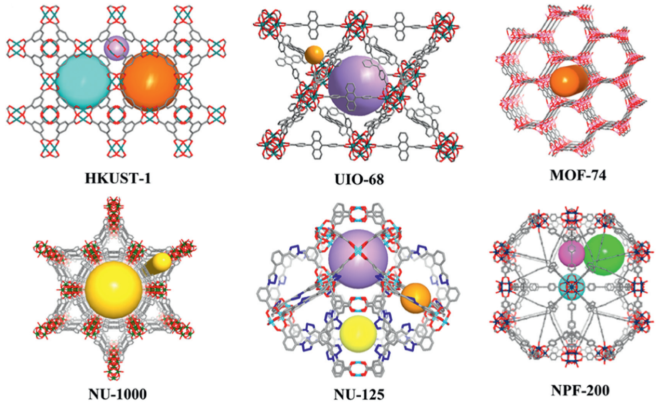

**Fig. 2.** Crystal structures of some representative MOFs. Reproduced with permission [34]. Copyright 2020, Wiley Publishing Group.

$NbOF_5^{2-}$ anion. Interestingly, NbOFFIVE-1-Ni has a higher $CO_2$ uptake (3.21 Å) than that of SIFSIX-3-Cu at 400 ppm [35]. These materials outperformed zeolite 13X and other representative MOFs such as UiO-66-$NH_2$ and Mg-MOF-74 (Fig. 3) [36].

For large-scale implementation of MOFs based sorbents, comprehensive evaluation of its performance under practical conditions including high humidity should be done [37], including long-term structural stability, performance in complex environments, and energy consumption during adsorbent regeneration, which should all be considered in place. In addition, the preparation cost and scalability of MOFs are also important factors [38]. Challenges for green synthesis in large scale also needs to be overcome, as only a few MOF can be prepared in large-scale currently [16,39]. Nevertheless, such emerging type of material brought great promise for DAC applications.

### *2.4. Carbon-based materials*

Porous carbon materials have the advantages of easy synthesis, high specific surface area [40], controllable pore size [41], high thermal stability [42], and low energy consumption for regeneration [43], which make them a very promising type of $CO_2$ capture sorbent. Among them, activated carbon is generally derived from biomass as a basic carbon material [44]. Balasubramanian *et al.* used the waste palm kernel shell as a carbon source, and prepared foam carbon with hierarchical pore structure by hydrothermal carbonization and pyrolysis for efficient selective $CO_2$ capture ($CO_2/N_2$ selectivity of 44) (Fig. 4). The adsorption of carbon dioxide by PKS-Lignin-P600 sample at 323 K, $P/P_0 = 0.005$ was about 1.43 mmol/g [45]. However, capturing carbon dioxide under a lower pressure is a challenging task, due to the weak physical interaction between the non-polar surface of carbon-based dsorbents and $CO_2$. Introduction of chemical functionalities including metal sites and basic sites on the pore surface might be a feasible approach to further promote its $CO_2$ adsorption.

### *2.5. Porous organic polymers*

Compared with porous carbon-based materials, MOF and zeolite sorbents, porous organic polymers (POPs) are usually prepared under stirring conditions which is favourable for large scale synthesis [46]. POPs also exhibit micro porosity, high specific surface area [47] and good chemical stability [48]. Their surface property can be improved by doping/functionalization to enhance the $CO_2$ adsorption. In addition, POPs usually hydrophobic, being suitable for DAC and post combustion capture under humid conditions [46]. For instance, Dai's group has developed a series of conjugated triazine framework HAT-CTFs-450/600 (hexaazatriphenylene-based conjugated triazine frameworks) for $CO_2$ capture under low partial pressure (0.15 bar/273 K, 3.0 mmol/g $CO_2$), based on an in situ doping strategy. The superior adsorption capacity among many POPs was attributed to the synergistic effect of its ultra-porous structure and element doping (Fig. 5) [49]. However, such performance is still not good enough for DAC application, as the adsorption capacity for ppm level $CO_2$ is very limited. Besides, efficient synthetic routes with cheap monomers need to be further explored [50].

Overall, significant progress has been made for $CO_2$ capture with physisorbents over the past decades. However, it is still quite challenging to gain high adsorption capacity under ultra-low pressure (400 ppm) that is relevant to DAC application, due to the relatively weak host-guest interactions. A few recent examples of fluorinated MOFs have shown great potential to promote the $CO_2$ uptake through efficient pore confinement and rich electronegative sites. These sorbents exhibit a relatively high $Q_{st}$ among physisorbents, while still lower than most chemisorbents (Table 2). The future research needs to further explore the adsorption/desorption kinetics and regeneration energy cost in comparison with chemisorbents.

## 3. Chemisorption materials

Chemical adsorption occurs when a chemical bond is formed between the sorbent and the sorbate [15]. Among various carbon dioxide capture technologies, liquid and solid sorbents based on alkali and alkaline earth metal oxides and hydroxides can easily react with carbon dioxide to form carbonates due to their high chemical binding energy [51]. Subsequently, carbon dioxide is released by heating the sorbent to a high temperature, and the heat loss during the regeneration process is quite significant [52]. This high regenerative energy consumption makes the operational cost of DAC very high [53]. In recent years, the alkylalcohol ammonia solution has been used at industrial operation scale [54,55]. Since 1930, primary and secondary amine aqueous solutions have been widely used to capture $CO_2$ from air at high partial pressure through chemical bonding between the Lewis acidic $CO_2$ and the basic amino group [56,57]. However, issues including their high regeneration energy, amine degradation, high heat capacity, and corrosion of equipment are difficult to be overcome, which has hindered their large-scale application [58].

In contrast, solid amine sorbents are considered to be promising alternatives for $CO_2$ capture from the air due to their non-corrosive, high $CO_2$ adsorption capacity and low regeneration energy consumption [59,60]. The chemisorbents used for DAC research are usually composed of amines supported on the porous solid matrix such as mesoporous silica, cellulose and MOFs [61]. The highly porous structure of support material enabled high loading of amine molecules and fast diffusion of $CO_2$ [62].

The preparation methods of amine-functionalized porous sorbents can be divided into three types (Fig. 6): (1) Physical impregnation; (2) Grafting through covalent or coordination bond; (3) *In-situ* polymerization of inorganic supports and amine-containing units [63]. In the following sections, we will discuss different types of amine loaded porous sorbents and their $CO_2$ capture performance.

### *3.1. Amine-loaded porous silica*

Porous silica materials, such as SBA-15 (Santa Barbara Amorphous well-ordered hexagonal mesoporous silica), MCM-41 (Mobil Composition of Matter No. 41) and KIT-n (Korea Advanced Institute of Science and Technology), have been regarded as promising sorbents for effective $CO_2$ capture after surface amino modification (Fig. 7) [64]. Especially under dry conditions, amines re-

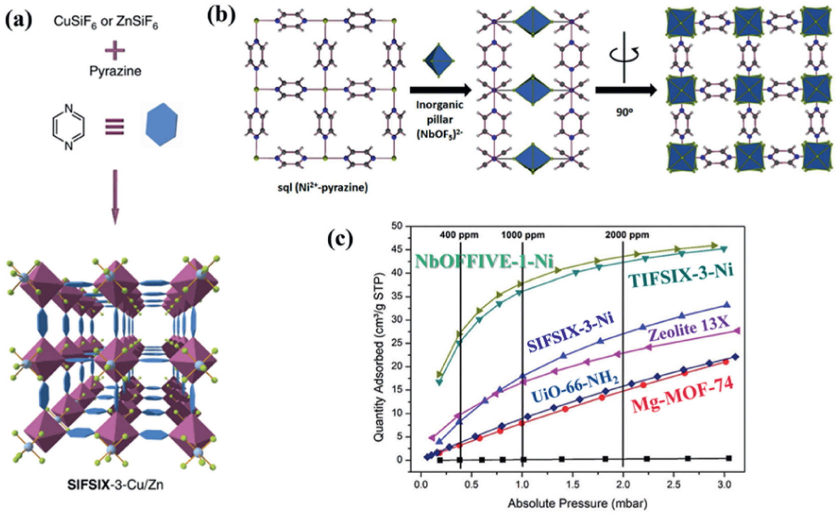

**Fig. 3.** (a) Synthesis and the channel structures of SIFSIX-3-Cu; (b) Structure view of NbOFFIVE-1-Ni along different directions; (c) $CO_2$ adsorption isotherms in the range 0 to 3000 ppm at 298 K of HKUST-1, Mg-MOF-74, SIFSIX-3-Ni, TIFSIX-3-Ni, Zeolite 13X, NbOFFIVE-1-Ni and UiO-66-$NH_2$. Reproduced with permission [17]. Copyright 2014, Springer Nature. Reproduced with permission [35]. Copyright 2016, American Chemical Society. Reproduced with permission [36]. Copyright 2017, Royal Society of Chemistry.

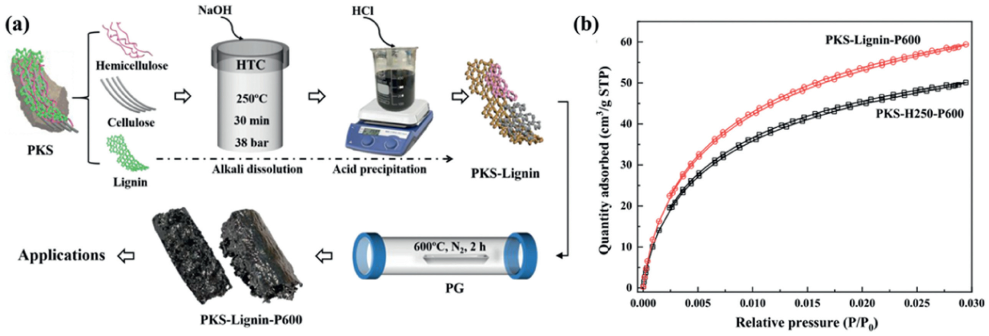

**Fig. 4.** (a) Schematic illustration for the synthesis of PKS-Lignin-P600; (b) $CO_2$ adsorption-desorption isotherms of PKS-H250-P600 and PKS-Lignin-P600. Reproduced with permission [45]. Copyright 2022, Elsevier.

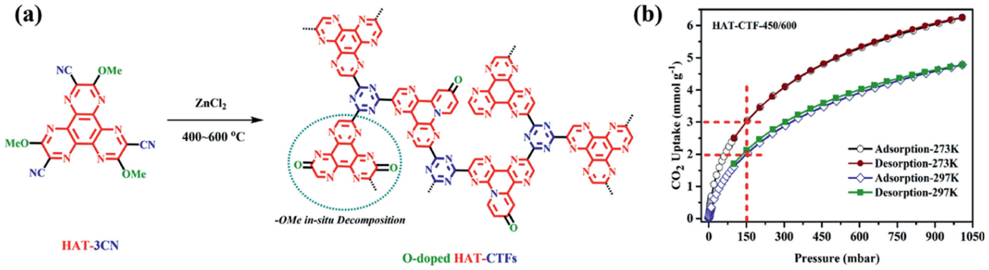

**Fig. 5.** (a) Synthesis route of proposed O-Doped HAT-CTFs; (b) $CO_2$ adsorption-desorption of HAT-CTF-450/600 at both 273 and 297 K. Reproduced with permission [49]. Copyright 2016, American Chemical Society.

act with $CO_2$ to form carbamates (zwitterionic mechanism), which greatly improves the adsorption capacity and selectivity of $CO_2$ [65,66]. The pioneering work of amine-impregnated silica porous sorbents for $CO_2$ capture was carried out by Song *et al.* who reported a material obtained by loading poly(ethylenimine) (PEI) on MCM-41 [67]. Afterwards, a large number of papers have been published on this topic, and the adsorption performance of the amine-loaded solid sorbents synthesized with different types of amine have been evaluated, including PEI, pentaethylaniline (PEHA), (3-aminopropyl)triethoxysilane (APTES) and tetraethylaniline (TEPA) [68–72]. The work of Sayari *et al.* [73] demonstrated that the triamine-grafted mesoporous silica TRI-PE-MCM-41 has high adsorption capacity (0.98 mmol/g) at low $CO_2$ partial pressure (400 ppm) in air, good stability and excellent $CO_2$ selectivity under dry and wet conditions.

### *3.2. Amine-modified metal-organic framework*

As a class of crystalline porous materials, MOFs have the advantages of adjustable chemical properties (pore size, structure, surface chemistry) and are very attractive for $CO_2$ capture [74]. In recent years, MOF-based sorbents have been rapidly developed, significant adsorption performance has been achieved for flue gas capture [75,76]. However, only limited number of MOF have reasonable adsorption capacity under very low partial pressure for DAC application [32]. A promising strategy is the post-synthetic

**Table 2**
Performance of representative porous sorbents for DAC capture.

| Class | Material | $Q_{st}$ (kJ/mol) | Adsorption condition | $CO_2$ uptake (mmol/g) | Ref. |
|---|---|---|---|---|---|
| Physisorbents | APG-III | – | 295 K, 400 ppm | 0.42 | [50] |
| | LTA ($Na^+$, $Ca^{2+}$, $Mn^{2+}$, $Ce^{3+}$) | 39 | 298 K, 350 ppm | 1.2 | [114] |
| | Na-GIS | – | 298 K, 400 ppm | 0.7 | [24] |
| | SIFSIX-3-Cu | 54 | 298 K, 0.4 mbar | 1.24 | [115] |
| | SIFSIX-2-Cu-i | 32 | 298 K, 0.4 mbar | 0.0684 | [24] |
| | SIFSIX-3-Zn | 45 | 298 K, 0.4 mbar | 0.13 | [24] |
| | TIFSIX-3-Ni | 55 | 298 K, 0.2 mbar | 0.71 | [24] |
| | SIFSIX-3-Ni | 44 | 298 K, 0.2 mbar | 0.18 | [17] |
| | SynAalumina | – | 298 K, 400 ppm | 1.74 | [116] |
| | NaCaA-85 | 52 | 298 K, 400 ppm | 1.8 | [117] |
| | MOR5 | 30 | 298 K, 400 ppm | 1.15 | [118] |
| | Zn-CHA2-1.9W2X | 42 | 303 K, 400 ppm | 0.67 | [119] |
| Chemisorbents | NbOFFIVE-1-Ni@polyacrylates | 56.2 | 298 K, 400 ppm | 1.44 | [120] |
| | MF-Cr-AEEA | – | 298 K, 400 ppm | 2.05 | [36] |
| | Ph-3-ED/SBA-15 | – | 308 K, 400 ppm | 0.92 | [121] |
| | Ph-6-PD/SBA-15 | – | 308 K, 400 ppm | 0.27 | |
| | $^{29}$Si CP/MASNMR (DT-grafted SBA-15) | – | 318 K, 400 ppm | 0.30–0.64 | [122] |
| | PEI-infused cellulose acetae-$SiO_2$ | – | 308/318/328 K, 395 ppm | 0.62/0.56/0.33 | [123] |
| | PEI/PME | – | 298 K, 400 ppm (0%–90% RH) | 2.2–2.9 | [124] |
| | ePTFE/silica | 67 | 308 K, 400 ppm | 1.62 | [125] |
| | PPN-6-$CH_2$ DETA | 60 | 295 K, 400 ppm | 1.04 | [126] |
| | PPN-6-$CH_2$EDA | 55.5 | 295 K, 0.05 bar | 1.70 | [127] |
| | PPN-6-$CH_2$TAEA | 40 | 295 K, 0.05 bar | 1.80 | [127] |
| | PP-2-DETA | 48.2 | 298 K, 0.05 bar | 0.74 | [128] |
| | P(DVB-co-VBC)-31-TEPA | 41 | 298 K, 0.05 bar | 0.79 | [129] |
| | Py-TMC-MA | 25.4 | 273 K, 0.05 bar | 0.98 | [130] |
| | PP1-2-TREN | 78 | 273 K, 0.05 bar | 1.13 | [131] |
| | PEI–$Mg_{0.55}$Al–O | – | 298 K, 400 ppm | 1.66 | [132] |
| | $Mg_{0.55}$Al-O-TEPA | – | 298 K, 400 ppm | 3 | [60] |

APG-III = Nax[$(AlO_2)_{86}(SiO_2)_{106}$]·x$H_2O$; LTA = Linde Type A zeolite; SIFSIX = $SiF_6{}^{2-}$; TIFSIX = $TiF_6{}^{2-}$; NaCaA-85 = $Ca^{2+}$-ion-exchanged A-type zeolite; MOR = mordenite-type zeolite; CHA = zinc containing chabazite zeolites; NbOFFIVE = $(NbOF_5)^{2-}$; MF-Cr-AEEA = *N*-(2-aminoethyl)ethanolamine (AEEA) with low volatility is applied to functionalize MIL-100(Fe), UiO-66(Zr), and MIL-100(Cr); PPN = porous polymer network; Ph-X-YY = alkyl-aryl amine-rich molecules; ED = ethylene diamine; PD = propane-1,3-diamine; PP-x = porous polymers; DVB = ivinylbenzene; VBC = 4-vinylbenzyl chloride; P(DVB-*co*-VBC)-31 = porous polymer; Py = perylene; TMC = trimesoyl chloride; MA = melamine; PP1-2-TREN = micro-/mesoporous polymers modified with tris(2-aminoethyl)amine.

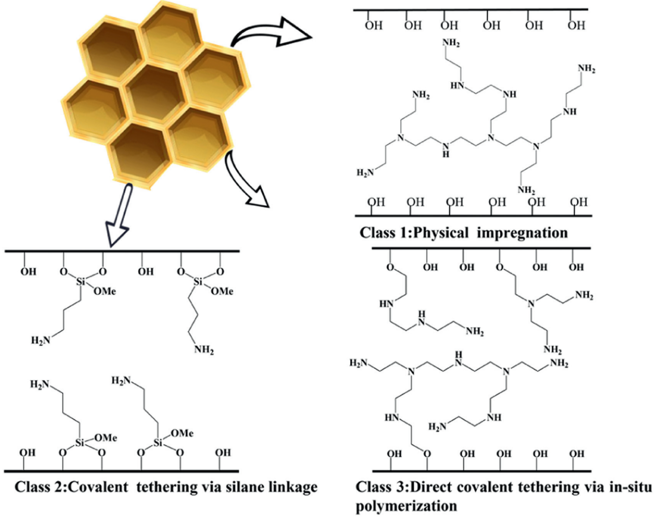

**Fig. 6.** Schematic diagram of three main strategies of amine functionalization of porous supports. Class 1 sorbent: polyethyleneimines (PEI) impregnated in porous materials. Class 2 sorbent: amines covalently tethered through silane linkages. Class 3 sorbent: *In situ* aziridine polymerization on a solid material.

functionalization of MOFs with alkanolamines as chemisorbents of carbon dioxide through the formation of zwitterionic carbamates or carbamates [77,78]. Multiple types of amines including ethylenediamine (EDA) [79,80], tris(aminoethyl)amine (TAEA) [81], TEPA [82], PEI [83], tris(2-amino ethyl) (TREN) [81] and PEHA [84] have been used for impregnation in Mg-MOF-74 [85,86], MIL-101 (Cr) [87], and HKUST-1 [88]. For instance, Long *et al.* [89] modified the $Mg_2$(dobpdc) material with ethylene diamine which showed high adsorption under 120 °C, being a promising candidate for temperature swing adsorption (TSA), as shown in Figs. 8a and b. Chen *et al.* [90] loaded the smallest diamine hydrozine molecule in classical $Mg_2$(dobdc) to achieve a high record capacity of 3.89 mmol/g at 0.4 mbar and 298 K (Figs. 8c and d).

Although MOF has a larger pore volume and specific surface area than other porous materials and has become a potential candidate for amination, due to its structural complexity and narrow pores, it may face the problem of blocking pore channels with high amine loading, which leads to poor adsorption kinetics [83]. Interestingly, a unique adsorption mechanism through cooperative $CO_2$ insertion between metal site and amine was discovered. Such novel mechanism enabled further tunability of adsorption behavior, for example, the strength of metal-amine coordination bonds plays an important role in controlling the adsorption step pressures [91,92].

### 3.3. Amine functionalized metal-oxide materials

Metal oxides are broadly used in the field of $CO_2$ capture due to their wide operating temperature, abundant source of raw materials and low price [93]. However, some metal oxides faced the challenges of poor stability, easy surface hardening and low adsorption capacity at high temperature or in the presence of water vapor [94,95]. In addition, the high energy consumption of the regeneration process is also a limit for the widespread use of metal oxides [96]. So far, a large number of studies have strived to increase the porosity of metal oxides [97,98] and modify the surface with amine [99,100] to promote the $CO_2$ adsorption capacity under low pressure. Taking advantage of the unique structure of

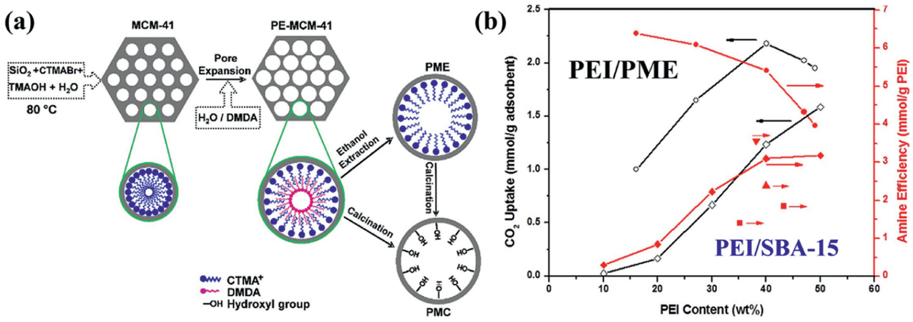

**Fig. 7.** (a) Model structure diagram of PEI loading in the pore-expanded MCM-41; (b) The $CO_2$ (400 ppm in $N_2$) uptake and amine efficiency at 25 °C as a function of PEI loading for PEI/PME(x), PEI/SBA-15, [PME = pore-expanded MCM-41 with a surface layer of cetyltrimethylammonium (CTMA) cations]. Reproduced with permission [64]. Copyright 2011, American Chemical Society.

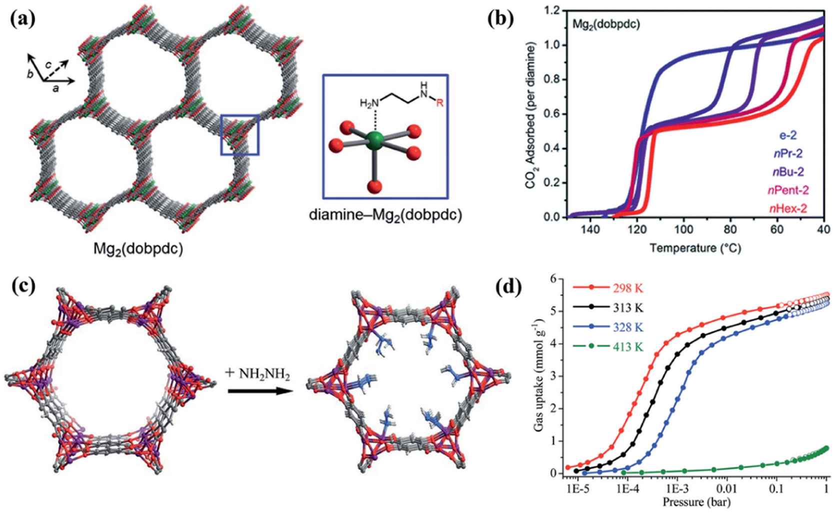

**Fig. 8.** (a) Structure of the MOF $Mg_2$(dobpdc) and ethylenediamine coordination at open metal site. (b) Pure $CO_2$ adsorption isobars of a series of $Mg_2$(dobpdc) variants loaded with various types of diamines. (c) Structures of [$Mg_2$(dobdc)] and [$Mg_2$(dobdc)($N_2H_4$)$_2$]. (d) $CO_2$ adsorption (solid) and desorption (open) isotherms measured at 298, 313, 328 and 413 K. Reproduced with permission [89]. Copyright 2016, Royal Society of Chemistry. Reproduced with permission [90]. Copyright 2018, Royal Society of Chemistry.

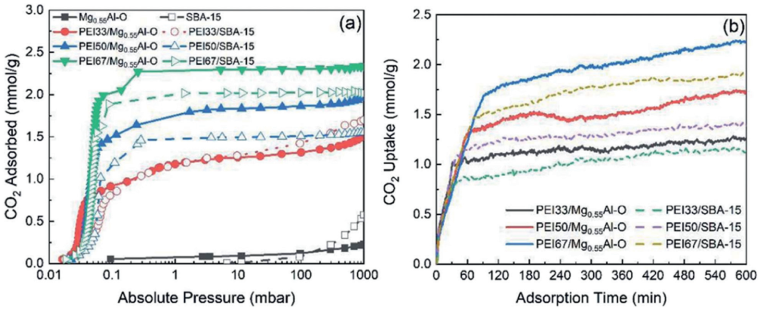

**Fig. 9.** (a) $CO_2$ adsorption isotherms of PEI/SBA-15 and PEI/$Mg_{0.55}$Al–O at 25 °C. (b) $CO_2$ adsorption kinetics of PEI-impregnated SBA-15 and $Mg_{0.55}$Al–O at 25 °C under 400 ppm $CO_2$. Reproduced with permission [101]. Copyright 2020, Royal Society of Chemistry.

layered double hydroxide (LDHs), Wang *et al.* prepared the mixed metal oxide (MMO) nanosheets from LDHs, and the nanosheet further formed spherical particles through self-assembly. The material contained abundant mesopores and surface defects to form strong interaction with amine molecules, and therefore prohibited the leakage of amine molecules during the regeneration process [101]. Up to 67 wt% of PEI was loaded in to Mg-Al-$CO_3$ LDH derived MMOs (Fig. 9). Thanks to the nanostructure of the MMOs, PEI is evenly dispersed on the surface, which improved the accessibility of $CO_2$ molecules to the amine adsorption sites. In addition, the sorbent has good thermal stability (up to 300 °C), which is mainly attributed to the strong electrostatic attraction between the MMO layer and the polyamines [101]. Finally, the material exhibits unexpected high adsorption capacity (2.27 mmol/g), fast kinetics and high stability under 25 °C and 0.4 mbar $CO_2$ conditions. This study demonstrated great promise of MMO sorbents by simple preparation methods with cheap raw materials for scalable DAC applications.

For practical DAC application using the amine-modified porous metal oxides, further studies are still needed. For the synthesis of different metal oxides, the process safety, simplicity and high repeatability need to be optimized to meet industrial standard. Most

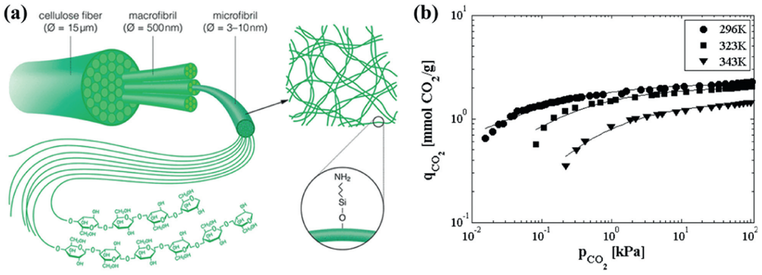

**Fig. 10.** (a) Preparation route of amine (APDES = 3-aminopropylmethyldiethoxysilane) modified NFC (nanofibrillated cellulose) adsorbent. (b) $CO_2$ adsorption isotherms of APDES-NFC at 296 K (●), 323 K (■), and 343 K (▼) as a function of $CO_2$ pressure and the numerically fitted Toth model (solid line). Reproduce with permission [105]. Copyright 2014, American Chemical Society.

of the sorbents studied at the present stage are in powder form, making them difficult for engineering in a pressure swing adsorption (PSA) or temperature swing adsorption (TSA) process. In the future, it is necessary develop strategies for material shaping in granular/columnar form. Comprehensive analysis of the influence of the type and concentration of organic amine during the loading process, could provide more insights on adsorption mechanism to further optimize the adsorption capacity and kinetics.

### 3.4. Amine-functionalized cellulose nanofiber

The traditional cellulose medium not only has high surface area and good water stability, but also has the advantages of abundant resources, renewable and easy degradation, which make it widely studied for wastewater treatment, drug release and gas adsorption [30,31,102,103].

Recently, the amine-functionalized cellulose nanofibers (CNFs) have been widely used in $CO_2$ adsorption studies. As a new advanced porous material, CNF has a series of outstanding characteristics, such as large aspect ratio, ecological friendliness, biocompatibility, light weight and rich hydroxyl groups for facile chemical modification [104,105]. For example, at 296 K and 0.02 kPa $CO_2$ partial pressure, Gebald *et al.* [105] analyzed the single-component $CO_2$ adsorption of amino-functionalized nanocellulose, showing a capture capacity of 0.85 mmol/g and an adsorption heat of −50 kJ/mol (Fig. 10). The results showed that the adsorption capacity of $CO_2$ increased dramatically by surface modification, especially with high loading of phthalimide. Jovanovic *et al.* [106] constructed a closed-loop experimental facility for direct air capture, and investigated the co-adsorption kinetics of carbon dioxide and water on a differential bed composed of amine-functionalized nanocellulose, the $CO_2$ adsorption capacity reached 1.25 mmol/g at 0.01 bar and 308 K.

Amino-functionalized nanocellulose has been adopted in commercial scale for carbon capture [106]. Due to their high availability, the annual production exceeds 100 million tons. In addition to being converted into cellulose derivatives, they can also be used to prepare cellulose nanocrystals (CNCs) [76]. Although nanocellulose display many advantages, in specific applications, it exhibits poor interfacial adhesion and excessive water sorption [75,107]. Further studies are suggested to be carried out, including stability during high temperature regeneration, retention of surface area after functionalization, and development of new cellulose-based sorbents. Besides, they can also be combined with other solid supports and leverage their strengths in order to promote DAC application.

### 3.5. Porous metal oxides

Since the 21st century, great progress has been made in the capture of $CO_2$ by porous metal oxides [95,108]. Among porous metal oxides, single and multi-component porous metal oxides ($Li_2O$, alkaline earth metal oxides, $TiO_2/CaO$) have been studied extensively [109]. MgO and CaO generally exhibit small specific surface area and pore volume and prone to form dense carbonate films with carbon dioxide and hinder the diffusion of $CO_2$ [110]. The sorbent regeneration is usually performed under high temperature, which causes high energy consumption. In addition, during the regeneration process, agglomeration sintering and pore shrinkage often happens, which deviate the adsorption capacity sharply during multiple cycles. Overall, porous metal oxides are more suitable for $CO_2$ capture under high temperature for certain industrial environment rather than DAC application [111].

Overall, chemisorbents generally exhibit high $CO_2$ uptake under low pressure, due to its high affinity towards $CO_2$. The properties of amine-modified sorbents depend on multiple factors including amine loading, amine type, amine site density, size of the amine molecule immobilized on the porous supports [59]. The major challenge for amine-modified sorbents is the high regeneration temperature that not only consumes large amount of energy, but also leads to volatilization and aggregation of amine species, resulting in clogging of the pores and shortening the sorbent life time [61].

### 3.6. Energy consumption for sorbent regeneration

The most important characteristics of porous adsorbents for DAC include adsorption capacity, adsorption kinetics, regeneration energy and cycle stability. Among them, the regeneration energy penalty is the largest cost source of DAC, and the equivalent energy demand of solid adsorption DAC system (supported by grid or fossil fuel combustion) ranges of 4.2–18.75 GJ/t-$CO_2$ [112,113]. Through a more comprehensive analysis of reported examples, it is evidenced that sorbents with high adsorption capacity generally demands large amount of energy for regeneration, which can be attributed to the strong $CO_2$ affinity induced high $Q_{st}$ (Table 2) [17,24,36,50,60,114–132] Therefore, there is a trade-off between the goals of high adsorption capacity and low regeneration energy. Moreover, kinetic factors [133] and thermal conductivity [134] are also important considerations to the energy cost, and fast desorption could save energy to a high extent.

Moreover, coupling the $CO_2$ adsorption and catalytic conversion processes within a single material is another appealing approach, which not only greatly reduces the overall construction cost of the equipment, but also eliminates the energy consumption of adsorbent regeneration and reduces the overall cost of the system.

## 4. Conclusion

Given the increasing threat of global warming, large-scale deployment of negative carbon emission technologies is an essential step in the near future. Direct air capture is a promising technology to minimize $CO_2$ emissions. Among various sorbents for this purpose, porous materials are attractive candidates. This review article summarized the recent progress and status of porous materials for DAC application with representative examples of each type of material. According to the adsorption mechanism, porous sorbents were classified as physisorbents and chemisorbents.

Due to the low $CO_2$ concentration in the atmosphere, efficient sorbents should exhibit significant $CO_2$ adsorption under low partial pressure (400 ppm or 0.4 mbar). For physisorbents, the adsorption under low $CO_2$ partial pressure is generally very limited. Only a few materials developed recently exhibit considerable $CO_2$ adsorption under 0.4 mbar. Given the highly tunable pore size and rich functional sites, MOFs materials are perhaps the most promising physisorbents. However, the moderate stability and high production cost of MOFs are grand challenges for their practical application in large scale. Alternatively, chemical adsorption of $CO_2$ is another feasible approach. The most popular amine-modified porous sorbent was synthesized by loading polyamines into porous supports. The strong interaction between amine sites and $CO_2$ led to high adsorption capacity under low pressure, however, the regeneration energy is also quite high. Besides, the high temperature may also cause amine degradation and irreversible decrease of adsorption capacity. In addition to the solid porous sorbents, porous liquids [135] with accessible permanent porosity and excellent processability [136] have been explored for gas separation including post-combustion $CO_2$ capture [137–139]. Porous liquids might also be excellent candidates for DAC if their affinity to $CO_2$ can be promoted to capture low concentration $CO_2$.

For practical application of these sorbents, other properties need to be considered, such as: long-term stability under practical conditions, recyclability, heat capacity and shaping. It is estimated that DAC sorbents should undergo at least tens of thousands of cycles, and reported materials are generally recycled less than 10 times. In addition, there are trade-offs between several key properties of the materials, such as adsorption capacity, selectivity, regeneration energy, resistance to moisture and high temperatures, economic costs.

In conclusion, DAC technology is still in its infancy. Its practical application in large scale relies on the development of advanced porous sorbent materials with high performance and low cost of production and operation. The fast development of porous materials for $CO_2$ capture would significantly flourish this field. It is expected that cost effective DAC technology will be readily available in the near future to contribute the carbon neutrality.

## Declaration of competing interests

The authors declare that they have no known competing financial interests or personal relationships that could have appeared to influence the work reported in this paper.

## Acknowledgments

We acknowledge financial support from the National Natural Science Foundation of China (Nos. 22278011, 22225803, 22038001 and 22108007). Beijing Natural Science Foundation (No. Z230023) The Science & Technology Project of Beijing Municipal Education Committee (No. KZ201810005004). Beijing Nova Program (No. Z211100002121094).

## References

[1] Z. Yang, C. He, H. Sui, L. He, X.G. Li, J. $CO_2$ Util. 30 (2019) 79–99.
[2] B. Parkinson, P. Balcombe, J.F. Speirs, A.D. Hawkes, K. Hellgardt, Energy Environ. Sci. 12 (2019) 19–40.
[3] M. Fajardy, N.M. Dowell, Energy Environ. Sci. 11 (2018) 1581–1594.
[4] S. Szima, S.M. Nazir, S. Cloete, et al., Renew. Sustain. Energy Rev. 110 (2019) 207–219.
[5] G.A. Meehl, T.F. Stocker, W.D. Collins, et al., Climate. Change 2007: The Physical. Science. Basis. Contribution of Working Group I to the Fourth Assessment Report of the Intergovernmental Panel on Climate Change. New York, 2007, pp. 749–844.
[6] A. Cherevotan, J. Raj, L. Dheer, et al., ACS Energy Lett. 6 (2021) 509–516.
[7] S. CastroPardo, S. Bhattacharyya, R.M. Yadav, et al., Mater Today 60 (2022) 227–270.
[8] K. Lackner, H.J. Ziock, P. Grimes, Los Alamos National Lab, United States, 1999.
[9] S. Kar, R. Sen, A. Goeppert, G.K. Surya Prakash, J. Am. Chem. Soc. 140 (2018) 1580–1583.
[10] J.F. Zheng, X.P. Chen, J.L. Ma, Clean Energy Sci. Technol. 1 (2023) 95–119.
[11] M. Steinberg, V.D. Dang, Energy Convers. Manag. 17 (1977) 97–112.
[12] IEA International Energy Agency (IEA), https://iea.blob.core.windows.net/assets/78633715-15c0-44e1-81-df-41123c556d57/Direct Air Capture: A key technology for net zero.pdf. 2023.
[13] B. Sreenivasulu, I. Sreedhar, P. Suresh, K.V. Raghavan, Environ. Sci. Technol. 49 (2015) 12641–12661.
[14] C.H. Yu, C.H. Huang, C.S. Tan, Aerosol Air Qual. Res. 12 (2012) 745–769.
[15] R.M. Firdaus, A. Desforges, A.R. Mohamed, B. Vigolo, J. Clean. Prod. 328 (2021) 129553.
[16] M. Oschatz, M. Antonietti, Energ Environ. Sci. 11 (2018) 57–70.
[17] O. Shekhah, Y. Belmabkhout, Z. Chen, et al., Nat. Commun. 5 (2014) 4228.
[18] L. Zou, Y. Sun, S. Che, et al., Adv. Mater. 29 (2017) 1700229.
[19] Y. Zeng, R. Zou, Y. Zhao, Adv. Mater. 28 (2016) 2855–2873.
[20] J. Přech, P. Pizarro, D.P. Serrano, J. Čejka, Chem. Soc. Rev. 47 (2018) 8263–8306.
[21] Q. Liu, A. MacE, Z. Bacsik, et al., Chem. Commun. 46 (2010) 4502–4504.
[22] P. Vasiliev, O. Cheung, Z. Bacsik, Zeolite type a sorbent: U.S. 2017, Patent Application, pp. 552.
[23] X.J. Xiang, T. Guo, Y.M. Yin, et al., Ind. Eng. Chem. Res. 62 (2023) 5420–5429.
[24] K.S. Kencana, K.C. Kemp, S.B. Hong, Sep. Purif. Technol. 329 (2024) 125154.
[25] J.Y. Wu, X.C. Zhu, Y.L. Chen, R.Z. Wang, T.S. Ge, Chem. Eng. J. 450 (2022) 137958.
[26] H. Azarabadi, K.S. Lackner, Appl. Energy 250 (2019) 959–975.
[27] N. Von Der Assen, P. Voll, M. Peters, A. Bardow, Chem. Soc. Rev. 24 (2014) 7982–7994.
[28] M.M. Sadiq, M.P. Batten, X. Mulet, et al., Adv. Sustain. Syst. 4 (2020) 2000101.
[29] L. Liu, H.L. Zhang, G.X. Wang, et al., J. Mater. Sci. 52 (2017) 9640–9647.
[30] H.C. Zhou, J.R. Long, O.M. Yaghi, Chem. Rev. 112 (2012) 673–674.
[31] N.T. Cervin, C. Aulin, P.T. Larsson, L. Wågberg, Cellulose 19 (2012) 401–410.
[32] S. Gaikwad, Y. Kim, R. Gaikwad, S. Han, J. Environ. Eng. 9 (2021) 1023.
[33] A. Sayari, Y. Belmabkhout, R. Serna-Guerrero, Chem. Eng. J. 171 (2011) 760–774.
[34] X. Zhang, R.B. Lin, J. Wang, et al., Adv. Mater. 32 (2020) 1907995.
[35] P.M. Bhatt, Y. Belmabkhout, A. Cadiau, et al., J. Am. Chem. Soc 138 (2016) 9301–9307.
[36] A. Kumar, C. Hua, D.G. Madden, et al., Chem. Commun. 53 (2017) 5946–5949.
[37] P. Li, H.C. Zeng, Environ. Sci. Technol. 51 (2017) 12998–13007.
[38] J.B. Lin, T.T.T. Nguyen, R. Vaidhyanathan, et al., Science 374 (2021) 1464–1469.
[39] H.T. An, X. Zhang, C. Dong, et al., Green Chem. Eng. 4 (2023) 64–72.
[40] T. Laing, C. Hen, X. Li, J. Zhang, Langmuir 32 (2016) 8042–8049.
[41] Takashi Kyotani, Carbon Alloys: Novel Concepts to Develop Carbon Science and Technology, Elsevier Science, 2003, pp. 109–127.
[42] Y. Li, X. Wang, M. Cao, J. $CO_2$ Util. 27 (2018) 204–216.
[43] M.L. Yang, L.P. Guo, G.S. Hu, et al., J. Am. Chem. Soc. 55 (2016) 757–765.
[44] O.H.P. Gunawardene, C.A. Gunathilake, K. Vikrant, S.M. Amaraweera, Atmosphere 13 (2022) 397.
[45] B. Zhang, Y. Jiang, R. Balasubramanian, Resour. Conserv. Recycl. 185 (2022) 106453.
[46] K.S. Song, P.W. Fritz, A. Coskun, Chem. Soc. Rev. 51 (2022) 9831–9852.
[47] D.J. Heldebrant, P.K. Koech, V.A. Glezakou, et al., Chem. Rev. 117 (2017) 9594–9624.
[48] Y.H. Abdelmoaty, T.D. Tessema, F.A. Choudhury, O.M. El-Kadri, H.M. El-Kaderi, ACS Appl. Mater. Interfaces 10 (2018) 16049–16058.
[49] X. Zhu, C. Tian, G.M. Veith, et al., J. Am. Chem. Soc. 138 (2016) 11497–11500.
[50] X. Wang, T. He, J. Hu, M. Liu, Environ. Sci. Nano 8 (2021) 890–912.
[51] E.S. Sanz-Perez, C.R. Murdock, S.A. Didas, C.W. Jones, Chem. Rev. 116 (2016) 11840–11876.
[52] V. Nikulshina, C. Gebald, A. Steinfeld, Chem. Eng. J. 146 (2009) 244–248.
[53] R.S. Liu, S. Xu, G.P. Hao, A.H. Lu, Chem. Res. Chin. Univ. 38 (2021) 18–30.
[54] A.S. Bhown, B.C. Freeman, Environ. Sci. Technol. 45 (2011) 8624–8632.
[55] N.E. Hadri, D.V. Quang, E.L.V. Goetheer, M.R.M. Abu Zahra, Appl. Energy 185 (2017) 1433–1449.
[56] K.S. Lakhi, G. Singh, S. Kim, et al., Micropor. Mesopor. Mater. 267 (2018) 134–141.
[57] G.T. Rochelle, Science 325 (2009) 1652–1654.
[58] H.M. Stowe, G.S.H. Wang, Ind. Eng. Chem. Res. 56 (2017) 6887–6899.
[59] M. Zhao, J. Xiao, W. Gao, Q. Wang, J. Energy Chem. 68 (2022) 401–410.
[60] B. Barkakaty, B.G. Sumpter, I.N. Ivanov, et al., Environ. Technol. Innov. 7 (2017) 30–43.
[61] L. Jiang, W. Liu, R.Q. Wang, et al., Prog. Energy Combust. 95 (2023) 101069.
[62] A.A. Azmi, M.A.A. Aziz, J. Environ. Chem. Eng. 7 (2019) 103022.
[63] G. Gómez-Pozuelo, E.S. Sanz-Pérez, A. Arencibia, et al., Micropor. Mesopor. Mater. 282 (2019) 38–47.
[64] A. Heydari-Gorji, Y. Belmabkhout, A. Sayari, Langmuir 27 (2011) 12411–12416.
[65] J. Yu, S.S.C. Chuang, Ind. Eng. Chem. Res. 56 (2017) 6337–6347.

[66] J. Jason, C.J. Lee, C.H. Yoo, et al., Langmuir 34 (2018) 12279–12292.
[67] X. Xu, C. Song, J.M. Andresen, Energy Fuels 16 (2002) 1463–1469.
[68] X. Guo, L. Ding, K. Kanamori, K. Nakanishi, H. Yang, Micropor. Mesopor. Mater. 245 (2017) 51–57.
[69] C. Ji, X. Huang, L. Li, et al., Materials 9 (2016) 835.
[70] R. Kishor, A.K. Ghoshal, Chem. Eng. J. 300 (2016) 236–244.
[71] D. Panda, S. Singh, E. Kumar, IOP Conf. Ser.: Mater. Sci. Eng. 377 (2018) 012148.
[72] E. Vilarrasa-Garcia, E.O. Moya, J. Cecilia, et al., Micropor. Mesopor. Mater. 209 (2015) 172–183.
[73] Y. Belmabkhout, R. Serna-Guerrero, A. Sayari, Chem. Eng. Sci. 65 (2010) 3695–3698.
[74] Y.S. Ok, D.C. Tsang, N. Bolan, J.M. Novak, Biochar from Biomass and Waste: Fundamentals and Applications, Candice, India, 2018.
[75] Y.C. Ng, L.Z. Yang, Z.R. Jovanovic, Ind. Eng. Chem. Res. 57 (2018) 13987–13998.
[76] N.A.D. Ho, C.P. Leo, Environ. Res. 197 (2021) 111100.
[77] S.K. Xian, Y. Wu, J.L. Wu, X. Wang, J. Xiao, Ind. Eng. Chem. Res. 54 (2015) 11151–11158.
[78] S. Xian, F. Xu, C. Ma, et al., Chem. Eng. J. 280 (2015) 363–369.
[79] A. Demessence, D.M. D'Alessandro, M.L. Foo, J.R. Long, J. Am. Chem. Soc. 131 (2009) 8784–8786.
[80] S. Choi, T. Watanabe, T.H. Bae, D.S. Sholl, W.J. Christopher, J. Phys. Chem. Lett. 3 (2012) 1136–1141.
[81] N. Wang, A. Mundstock, Y. Liu, A.S. Huang, J. Caro, Chem. Eng. Sci. 124 (2015) 27–36.
[82] X. Wang, H. Li, X.J. Hou, J. Phys. Chem. C 116 (2012) 19814–19821.
[83] L.A. Darunte, A.D. Oetomo, K.S. Walton, D.S. Sholl, W.J. Christopher, ACS Sustain. Chem. Eng. 4 (2016) 5761–5768.
[84] M. Anbia, V. Hoseini, J. Nat. Gas Chem. 21 (2012) 339–343.
[85] W.S. Drisdell, R. Poloni, T.M. McDonald, et al., Phys. Chem. Chem. Phys. 17 (2015) 21448–21457.
[86] T.M. McDonald, W.R. Lee, J.A. Mason, et al., J. Am. Chem. Soc. 134 (2012) 7056–7065.
[87] Y. Lin, H. Lin, H. Wang, et al., J. Mater. Chem. A 2 (2014) 14658–14665.
[88] C. Montoro, E. Garcia, S. Calero, et al., J. Mater. Chem. 22 (2012) 10155–10158.
[89] P.Q. Liao, X.W. Chen, S.Y. Liu, et al., Chem. Sci. 7 (2016) 6528–6533.
[90] P.J. Milner, J.D. Martell, R.L. Siegelman, et al., Chem. Sci. 9 (2018) 160–174.
[91] R.L. Siegelman, T.M. McDonald, M.I. Gonzalez, et al., J. Am. Chem. Soc. 139 (2017) 10526–10538.
[92] E.J. Kim, R.L. Siegelman, H.Z.H. Jiang, et al., Science 369 (2020) 392–396.
[93] P. Yang, D. Zhao, D.I. Margolese, B.F. Chmelka, G.D. Stucky, Nature 396 (1998) 152–155.
[94] L.M. He, W.L. Jiang, J.C. Li, Petrol. Sci. Technol. 51 (2022) 83–91.
[95] T.M. GüR, Prog. Energy Combust. Sci. 89 (2022) 100965.
[96] S. Lee, S. Park, J. Ind. Eng. Chem. 23 (2015) 1–11.
[97] G. Wang, Y. Guo, J. Yu, et al., Chem. Eng. J. 428 (2022) 132110.
[98] Y. Guo, C. Tan, Wang P, et al., Chem. Eng. J. 379 (2020) 122277.
[99] A.M. Alkadhem, M.A.A. Elgzoly, S.A. Onaizi, J. Environ. Chem. Eng. 8 (2020) 103968.
[100] A.M. Alkadhem, M.A.A. Elgzoly, A. Alshami, S.A. Onaizi, Colloids Surf. A 616 (2021) 126258.
[101] X.C. Zhu, T.S. Ge, F. Yang, et al., J. Mater. Chem. A 8 (2020) 16421–16428.
[102] A. Lund, G.V. Manohara, A.Y. Song, et al., Chem. Mater. 34 (2022) 3893–3901.
[103] C.A. García-González, M. Alnaief, I. Smirnova, Carbohyd. Polym. 86 (2011) 1425–1438.
[104] N. Li, W. Chen, G. Chen, X.F. Wan, J.F. Tian, ACS Sustain. Chem. Eng. 6 (2018) 6370–6377.
[105] C. Gebald, J.A. Wurzbacher, A. Borgschulte, Environ. Sci. Technol. 48 (2014) 2497–2504.
[106] H. Sehaqui, M. E.Gálvez, V. Becatinni, et al., Environ. Sci. Technol. 49 (2015) 3167–3174.
[107] K. Oksman, Y. Aitomäki, A.P. Mathew, et al., Compos. Part A 83 (2016) 2–18.
[108] X. Yang, S.K. Biswas, J. Han, et al., Adv. Mater. 33 (2021) 2002264.
[109] Y. Wang, B. Liu, X.A. Zhao, et al., Nat. Commun. 9 (2018) 4058–4065.
[110] M.T. Dunstan, F. Donat, A.H. Bork, C.P. Grey, C.R. Müller, Chem. Rev. 121 (2021) 12681–12745.
[111] Y. Hu, Y. Guo, J. Sun, H.L. Li, W.Q. Liu, J. Mater. Chem. A 7 (2019) 20103–20120.
[112] J. Elfving, J. Kauppinen, M. Jegoroff, et al., Chem. Eng. J. 404 (2021) 126337.
[113] K.J. An, K. Li, C.M. Yang, J. Brechtl, K. Nawaz, J. $CO_2$ Util. 76 (2023) 102587.
[114] S.M.W. Wilson, F.H. Tezel, Ind. Eng. Chem. Res. 59 (2020) 8783–8794.
[115] M. Guo, H. Wu, L. Lv, et al., ACS Appl. Mater. Interfaces 13 (2021) 21775–21785.
[116] A. Oda, S. Hiraki, E. Harada, et al., J. Mater. Chem. A 9 (2021) 7531.
[117] W. Chaikittisilp, H.J. Kim, C.W. Jones, Energy Fuels 25 (2011) 5528–5537.
[118] D.L. Fu, Y. Park, M.E. Davis, PNAS 119 (2022) e2211544119.
[119] D.L. Fu, Y. Park, M.E. Davis, Angew. Chem. Int. Ed. 61 (2022) e202112916.
[120] C. Chen, Q. Jiang, H. Xu, Z. Lin, Ind. Eng. Chem. Res. 58 (2019) 1773–1777.
[121] A.M. Wright, Z. Wu, G. Zhang, et al., Chem 4 (2018) 2894–2901.
[122] D.R. Kumar, C. Rosu, A.R. Sujan, et al., ACS Sustain. Chem. Eng. 8 (2020) 10971–10982.
[123] E.S. Sanz-Pérez, A. Fernández, A. Arencibia, G. Calleja, R. Sanz, Chem. Eng. J. 373 (2019) 1286–1294.
[124] A. Sujan, S.H. Pang, G. Zhu, C.W. Jones, R.P. Lively, ACS Sustain. Chem. Eng. 7 (2019) 5264–5273.
[125] A. Sayari, Q. Liu, P. Mishra, ChemSusChem 9 (2016) 2796–2803.
[126] J.M. Youn, G. Arvind, J.R. Matthew, C.W. Jones, ACS Appl. Mater. Interfaces 14 (2022) 40992–41002.
[127] W. Lu, J.P. Sculley, D. Yuan, et al., Angew. Chem. Int. Ed. 51 (2012) 7480.
[128] Y. Yang, C.Y. Chuah, T.H. Bae, Chem. Eng. J. 358 (2019) 1227.
[129] D. Lee, C. Zhang, H. Gao, Macromol. Chem. Phys. 216 (2015) 489.
[130] L. Wang, Q. Xiao, D. Zhang, et al., ACS Appl. Mater. Interfaces 12 (2020) 36652.
[131] C. Xu, Z. Bacsik, N. Hedin, J. Mater. Chem. A 3 (2015) 16229.
[132] W.G. Lu, J.L.P. Sculley, D.Q. Yuan, R. Krishna, H.C. Zhou, J. Phys. Chem. C 117 (2013) 4057–4061.
[133] J. Young, F. Mcilwaine, B. Smit, S. Garcia, M. van der Spek, Chem. Eng. J. 456 (2023) 141035.
[134] S.M. Moosavi, B.Á. Novotny, D. Ongari, et al., Nature 21 (2022) 1419–1425.
[135] N. O'Reilly, N. Giri, S.L. James, Chem. Eur. J. 13 (2007) 3020–3025.
[136] T.D. Bennett, F.X. Coudert, S.L. James, A.I. Cooper, Nat. Mater. 20 (2021) 1179–1187.
[137] H. Mahdavi, S.J.D. Smith, X. Mulet, M.R. Hill, Mater. Horiz. 9 (2022) 1577–1601.
[138] Y. Ding, L. Ma, X. Yang, et al., Energy 263 (2023) 125742.
[139] D.C. Wang, Y.P. Ying, Y.Y. Xin, et al., Acc. Mater. Res. 4 (2023) 854–866.